Aerodynamic Analysis of Helicopter Rotor by Coupling of CFD and Trim Calculation

Natsuki KONDO*1 , Tomoka TSUJIUCHI*1 , Hideaki NAKAMURA*1

Takashi AOYAMA*2 , Shigeru SAITO*2

Abstract

An iterative coupling method between an aerodynamic code based on the lifting-line theory and a computational fluid dynamics (CFD) code is developed and applied to the aerodynamic analysis of helicopter rotor. In this method, a comprehensive integral rotor code, CAMRAD II, and an unsteady Euler code are used as the aerodynamic and the CFD code respectively. This method is applied to the calculation of rotor aerodynamics in a high-speed forward flight condition and a descending flight condition. The calculated pressure distributions on the blade surface are in good agreement with experimental data in the high-speed forward flight case. In this case, analyses are conducted not only for a rectangular tip shape but also for simply modified tip shapes. It is indicated that the coupling method is required for the calculation of modified tip shapes. In the descending flight case, it is also shown that the present method is required. In addition, the acoustic pressure of blade-vortex interaction (BVI) noise is calculated. It is indicated that the coupling method is not always required for the prediction of BVI noise in this case.

1. Introduction

The aerodynamic code based on the lifting-line theory has been conventionally used to predict the performance and the trim condition of a helicopter rotor. Such an integral code cannot accurately predict the complex non-linear flow around a rotor in high-speed forward flight. For the prediction of such a transonic flow, CFD techniques have the advantage over other methods. However, CFD techniques have not yet captured the vortex dynamics of a helicopter rotor accurately.

Therefore, the aerodynamic analysis of a helicopter rotor in recent years is conducted by coupling a CFD code with a trim code based on the potential theory. The authors have conducted the rotor aerodynamic analysis by coupling an unsteady Euler code[1] with CAMRAD II. CAMRAD II is a comprehensive analytical code for the aerodynamics and dynamics of helicopters and it is based on the lifting-line theory. The sectional load and moment calculated in CAMRAD II are based on 2-D airfoil characteristics obtained by wind tunnel test. The rotor wake is modeled by discrete vortex elements. The inflow induced by the rotor wake is computed by Biot-Savart integration and the blade structural motion is estimated by the beam theory.

The inflow and the blade motion calculated by CAMRAD II are used to modify the boundary condition in the Euler calculation. Such an one-way coupling method is efficient from the view point of calculation time, but the airloads calculated by the CFD code and CAMRAD II do not always coincide. Therefore, an iterative coupling technique between two codes is proposed by C.Tung et al[2] in order to reduce the discrepancy of the airloads. They used a full potential CFD code. However, such a potential code is not sufficient to capture the generation and behavior of shock wave accurately. Therefore, a three-dimensional unsteady Euler solver is employed in this study.

2. Coupling Procedure

The communication between CAMRAD II and the unsteady Euler code is based on the partial angle of attack, α_p, and the prescribed increments in section lift coefficients, ΔC_L (see Figure 1).

The partial angle of attack is calculated by CAMRAD II excluding the effect of the wake elements inside of the Euler computational domain in order to avoid the double count of the effect. The tip vortex going across the computational domain is not considered in the Euler calculation because the computational domain wraps not the entire rotor but only one blade. The effect of the tip vortex is included in the computation of partial angle of attack. The calculated partial angle of attack is transferred to the unsteady Euler code to modify the boundary condition on the blade surface.

The computational domain of the Euler calculation is shown in Figure 2. The boundary

*1 Advanced Technology Institute of Commuter-helicopter
*2 National Aerospace Laboratory

shape of the domain is a box type. An O-H type grid is used and the number of grid is 77x50x51. 77 grid points are distributed in the airfoil's wrap around direction and 51 grid points are distributed between the blade surface and the far-field boundaries. There are 50 radial grid stations with 25 stations on the blade surface. The far-field boundaries are located at 7-chord away from the quarter-chord line of the blade. The boundaries in the spanwise direction are located at 0.4R and 1.5R.

The lift coefficient increment, ΔC_L, is defined as the difference between the section lift coefficients obtained by CAMRAD II and the unsteady Euler code. This increment is used to improve the trim solution of CAMRAD II. The increment lift coefficient is applied only in the region of the advancing side because the lift coefficient obtained by the Euler code is more accurate than that by CAMRAD II in this region. The region of the communication between CAMRAD II and the Euler code is checked by the two cases shown in Figure 3. The difference between the two cases is negligible, so following all calculations are conducted using the communication region of case A.

Figure 4 shows the flow chart of the iteration procedure. This procedure is repeated until the lift coefficient increments become almost zero.

3. Results

This method is applied to the calculation for the 1/7-scale AH-1G Operational Loads Survey (OLS) model rotor. The rotor characteristics are shown in Figure 5. This rotor has two teetering rectangular blades with linear twist and a symmetrical airfoil. In this study, the blade is assumed to be rigid. The calculation cases are shown in Table 1. Two operating conditions are chosen for this study. One of them is a high-speed forward flight condition and the other is a descending flight condition. In the high-speed forward flight case, analyses are conducted not only for a rectangular tip shape but also for simply modified tip shapes. One of them is the blade with a swept-back tip shape and the other is that with a tapered tip shape. The swept-back angle is 30 degrees and the taper ratio is 0.333. Both modifications start from 0.9R. The quantity R is the rotor radius.

3.1 High-speed forward flight

Figure 6 shows the evolution of the lift coefficient distribution with iteration number, N, at the azimuthal position of 90 degrees. The dashed line indicates the lift coefficient obtained by CAMRAD II and the solid line indicates that obtained by the Euler code. The initial solution calculated by CAMRAD II is shown in the figure of N=0. It is observed that the difference between the coefficients are reduced as the iteration number increases. The solution is almost converged after three-time iterations.

Figure 7 shows the measured[5] and calculated pressure distributions on the blade upper surface at N=1 and N=3. The comparisons are performed at the spanwise station of 0.95R at three azimuthal positions. It is indicated that the effect of the iteration is not clearly observed in the pressure distributions but the shock waves predicted by our Euler code is in good correlation with the experimental data.

Figures 8 and 9 show the evolution of the lift coefficient distribution with iteration number for the blade with the modified tip shapes at the azimuthal position of 90 degrees. The initial differences between the lift coefficients obtained by CAMRAD II and the Euler code are larger than that of the rectangular blade. In both cases, the difference is reduced after three iterations. The effect of the tip-shape modification is observed around 0.9R in the result of the Euler calculation. The effect of the swept-back tip shape is larger than that of the tapered tip shape. The pressure contours around the blade tips shown in Figure 10 clearly show the effect.

3.2 Descending flight

The present method is also applied to the calculation of a descending flight case. Figure 11 shows the evolution of the lift coefficient distribution with iteration number at the azimuthal position of 90 degrees. The effect of the blade-vortex interaction is observed both in the distributions obtained by CAMRAD II and the Euler code. Figure 11 shows that the present method is required for the descending flight condition.

In addition, the acoustic pressure of blade-vortex interaction (BVI) noise generated in this decsending flight condition is calculated using the present method. BVI is defined as the interaction between the blade and the tip vortices shed from the own blade or the preceding blades. Figure 12 shows the measured[7] and calculated acoustic waveforms of BVI noise. The calculations are preformed by an aeroacoustic code based on Ffowcs Williams and Hawkings (FW-H) formulation[6]. In this calculation, the pressure distribution on the blade surface obtained by the unsteady Euler code is used as noise sources. Both of the calculated waveforms accurately predict the number of positive peak although the values of the peak pressure are not exactly predicted. The difference between the calculated results of N=1 and N=3 is not remarkable. Therefore, the coupling method is not always required

for the prediction of BVI noise in this case.

4. Conclusions

An iterative coupling method between an aerodynamic code based on the lifting-line theory and a computational fluid dynamics (CFD) code is developed and applied to the aerodynamic analysis of the OLS model rotor in a high-speed forward flight and a descending flight conditions. For each cases, the convergence of this method is obtained after three iterations. It is indicated that the iterative procedure is required in the calculations of modified tip shapes in the high-speed forward flight condition. In the descending flight condition, it is shown that the present method is required but the predicted BVI noise is not strongly affected by the iteration procedure in this case.

References

(1) Aoyama, T. et al., Calculation of Rotor Blade-Vortex Interaction Noise Using Parallel Super Computer, 22nd European Rotorcraft Forum, 1996, pp.81.1-11.

(2) Tung, C. et al., The Prediction of the 40th Annual National Forum of AHS, 1984, pp.389-399.

(3) Strawn, R. C. et al, An Improved Three-Dimensional Aerodynamics Model for Helicopter Airloads Prediction, AIAA Paper 91-0767, 1991

(4) Aoyama, T. et al., Effect of Blade-Tip Planform on Shock Wave of Advancing Helicopter Blade, Journal of Aircraft, vol.32, No.5, Sep.-Oct. 1995, pp.955-961.

(5) Boxwell, D. A. et al., Model Helicopter Rotor High-Speed Impulsive Noise: Measured Acoustics and Blade Pressures, NASA TM-85850, 1983.

(6) Nakamura, Y. et al., Rotational Noise of Helicopter Rotors, Vertica, vol.3, no.3/4, 1979, pp.293-316.

(7) Splettstoesser, W. R. et al., Helicopter Model Rotor Blade Vortex Interaction Impulsive Noise: Scalability and Parametric Variations, 10th European Rotorcraft Forum, Paper Nr.18, 1984.

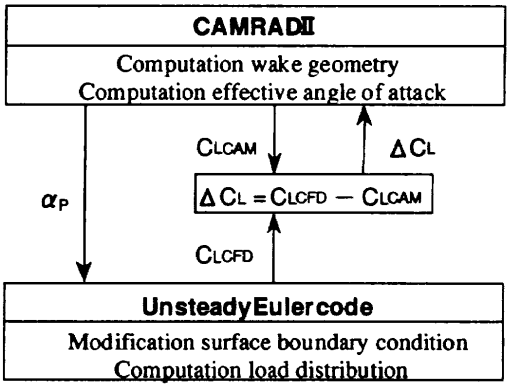

α_P : partial angle of attack excluding effect of wake vorticityin computational domain of CFD
ΔC_L : prescribed lift coefficient increment
C_{LCAM}: lift coefficients calculated by CAMRADII (without increment)
C_{LCFD}: lift coefficients calculated byEuler code

Figure 1 Procedure of iteration between CAMRADII and unsteady Euler code.

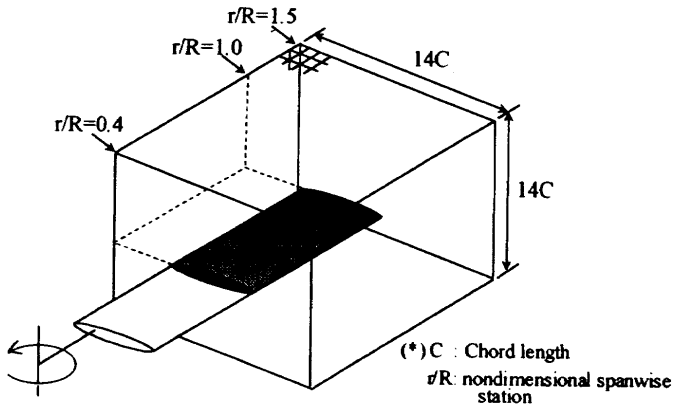

Figure 2 Computational domain for Euler calculation.

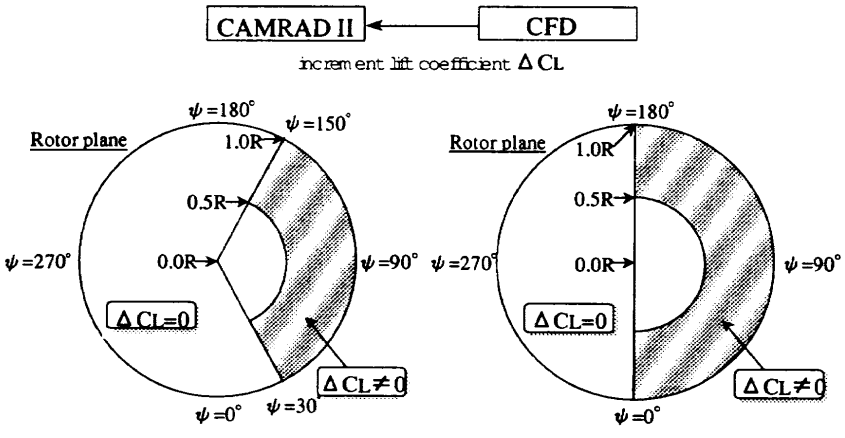

Figure 3 Communication region.

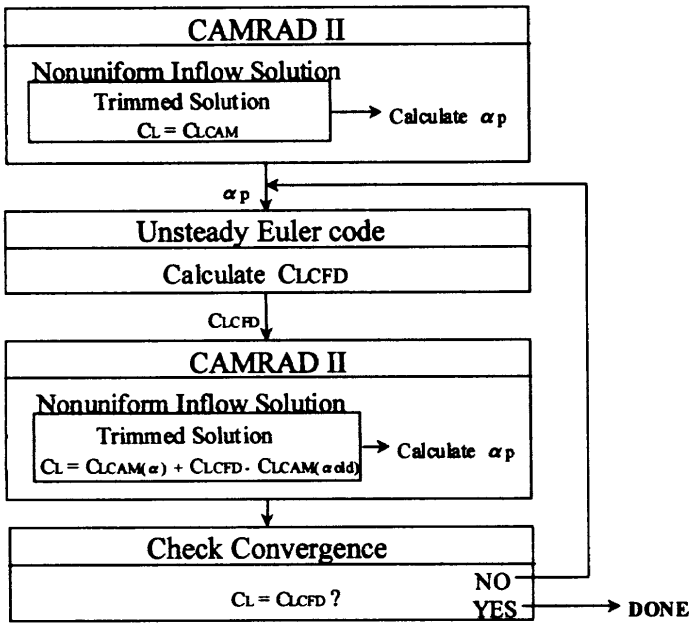

Figure 4 Flow of coupling method.

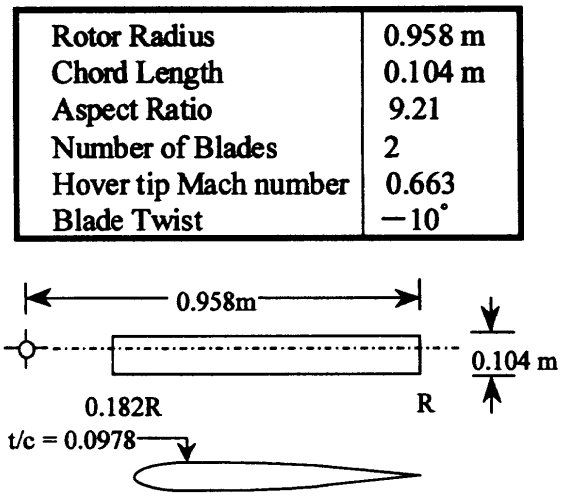

Figure 5 Rotor characteristics

Table 1 Calculation cases.

Tip planform	μ	α_{tpp}	C_T/σ
	0.298	-4.5°	0.0769
r/R=0.9, 30°			
r/R=0.9			
	0.164	+2.0°	

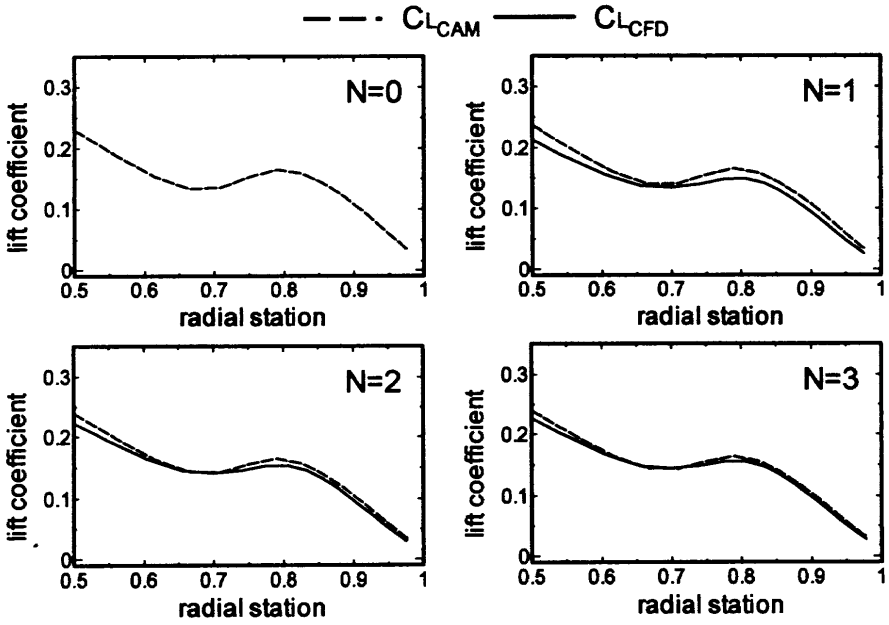

Figure 6 Evolution of lift coefficients (M_{tip}=0.663, μ=0.298).

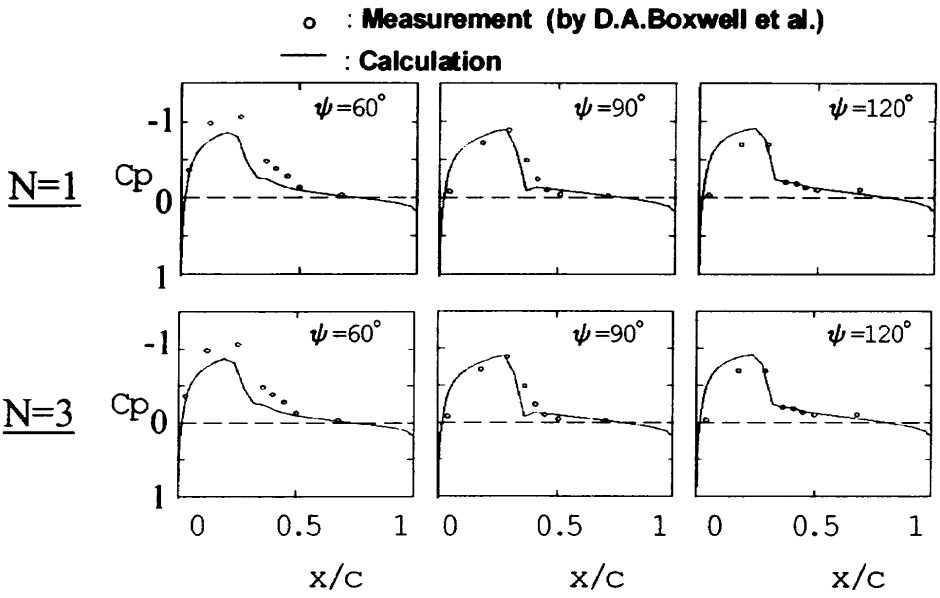

Figure 7 Pressure distributions on blade upper surface ($r/R=0.95$, $M_{tip}=0.663$, $\mu=0.298$).

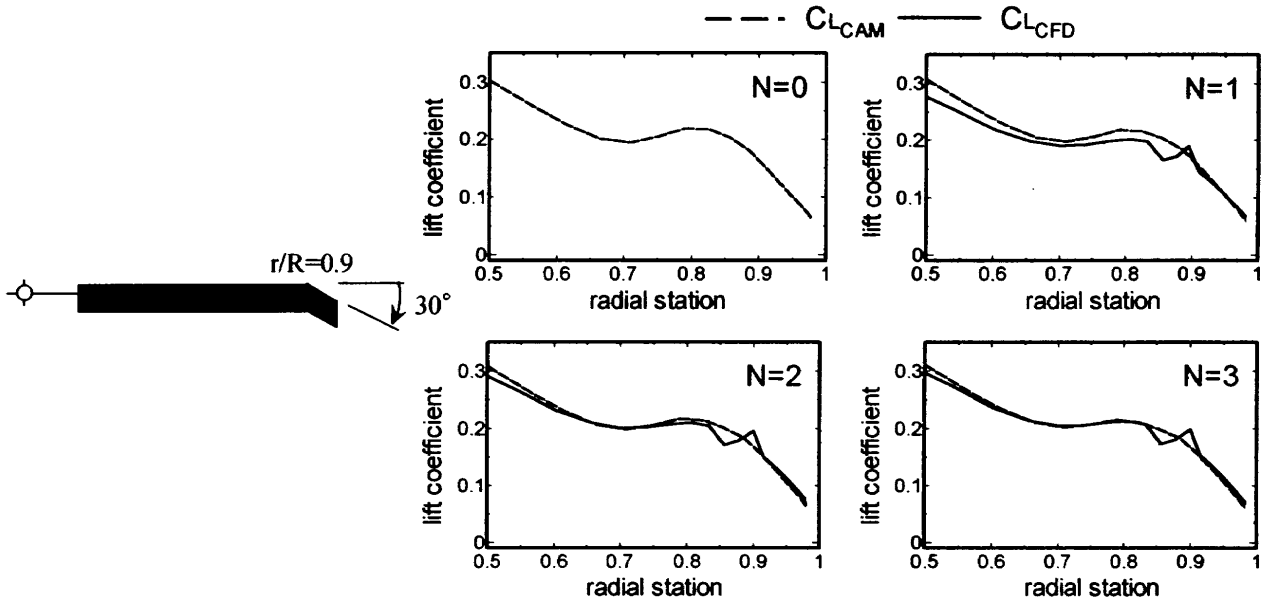

Figure 8 Evolution of lift coefficients ($M_{tip}=0.663$, $\mu=0.298$).

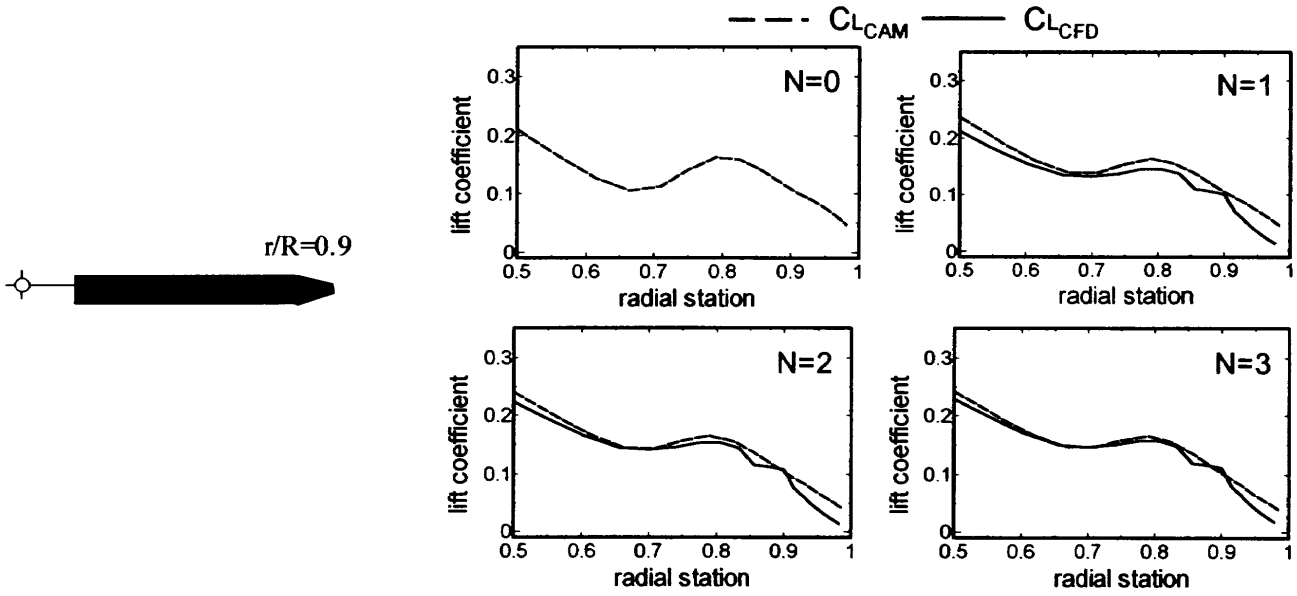

Figure 9 Evolution of lift coefficients ($M_{tip}=0.663$, $\mu=0.298$).

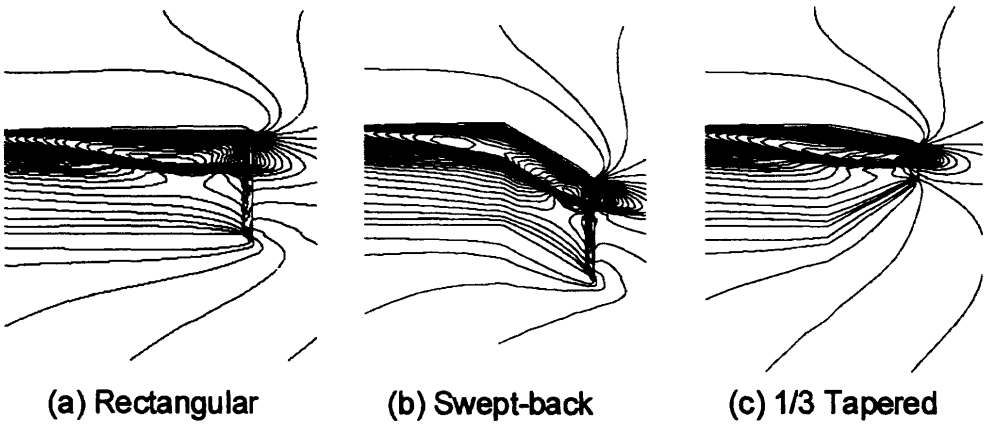

Figure 10 Pressure contours around three kinds of blade tip.

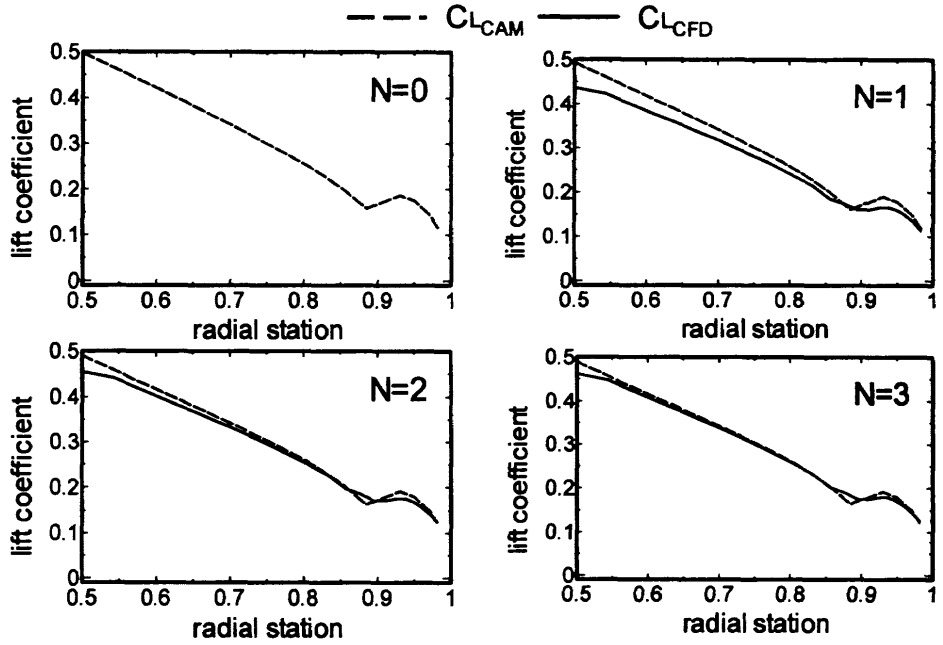

Figure 11 Evolution of lift coefficients (M_{tip}=0.663, μ=0.164, α_{tpp}=2°).

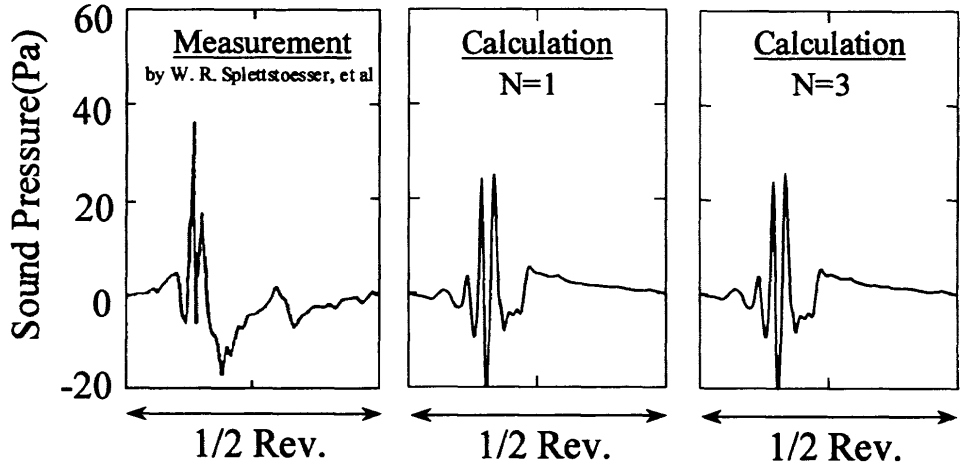

Figure 12 Iteration effect for BVI noise prediction.